Self-assembly of poly(vinylidene fluoride)-*block*-poly(2-(dimethylamino)ethylmethacrylate) block copolymers prepared by CuAAC click coupling

*Marc Guerre,[a] Mona Semsarilar,[b] Cedric Totée,[c] Bruno Améduri,[a] Vincent Ladmiral[a]**

SUPPORTING INFORMATION

M_n Calculation:

PVDF

$$(S1)\quad DP = \frac{\int_{2.70}^{3.19} \mathrm{CH_2\ (HT)} + \int_{2.28}^{2.43} \mathrm{CH_2 (TT)} + \int_{4.37}^{4.52} \mathrm{CH_2 (End-group)}}{2/3 \times \int_{1.19}^{1.24} \mathrm{CH_3\ (R-CTA)}}$$

$$(S2)\quad M_{nNMR} = M_nCTA + DP \times M_nVDF$$

With $M_{n\ CTA}$ = 263.33 g.mol^{-1} and $M_{n,VDF}$ = 64.04 g.mol^{-1}

PDMAEMA

$$(S3)\quad DP = \frac{\int_{3.93}^{4.16} \mathrm{CH_2\ (PDMAEMA)}}{\int_{4.59}^{4.68} \mathrm{CH_2\ (Initiator)}}$$

$$(S4)\quad M_{nNMR} = M_nCTA + DP \times M_nVDF$$

With $M_{n\ Initiator}$ = 205.05 g.mol^{-1} and $M_{n,DMAEMA}$ = 157.21 g.mol^{-1}

Functionality Calculation:

$$F = \frac{[X1]_0}{[X1]_0 + df([I]_0 - [I]_t)} \quad (S5)$$ [1]

$$[I]_0 - [I]_t = [I]_0\,(1 - e^{-k_d t}) \quad (S6)$$

With

$$k_d = A \times e^{-Ea/_{RT}} \quad (S7)$$

$$k_d = 1.77E^{+15} \times e^{-\frac{132.11E^{+3}}{8.314 \times 346.15}} = \mathbf{2.05\ E^{-5}\ s^{-1}}$$

$A = 1.77E^{+15} s^{-1}, Ea = 132.11\ kJ.mol^{-1}, R = 8.314\ J.mol^{-1}K^{-1}, K = 273.15 + 73 = 346.15\ K$

And

$$[I]_0 = 0.0104\ mol.L^{-1}, [X1]_0 = 0.104\ mol.L^{-1}$$

$$[I]_0 - [I]_t = [I]_0\,(1 - e^{-k_d t})$$

$$[I]_0 - [I]_t = 0.0104 \times \left(1 - e^{-2.05E^{-5} \times 24 \times 60 \times 60}\right) = \mathbf{8.63\ E^{-3} mol.L^{-1}}$$

$$F = \frac{[X1]_0}{[X1]_0 + df([I]_0 - [I]_t)}$$

$$F = \frac{0.104}{0.104 + 0.5(8.63E^{-3})} = \mathbf{0.96} \equiv \mathbf{96}\ \%$$

d and f were arbitrary defined to 1 and 0.5, respectively, corresponding to a simplified model without termination reactions and a relative moderate efficiency of the initiator.

F is the percentage of functionality or living chains, $[X1]_0$ the concentration of CTA, d = number of chains produced by termination, f initiator efficiency, and $[I]_0$-$[I]_t$ the concentration of generated radicals.

PVDF$_{40}$-*b*-PDMAEMA$_{23}$

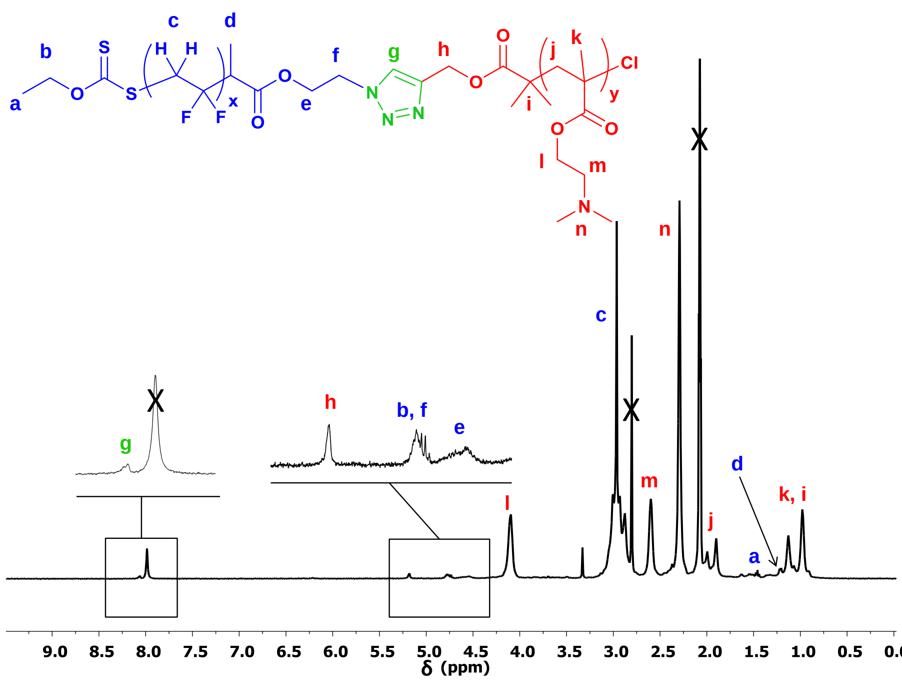

Figure S1. [1]H NMR spectrum in $(CD_3)_2CO$ of PVDF$_{40}$-*b*-PDMAEMA$_{23}$ BCP. The crossed-out peaks were assigned to residual $(CH_3)_2CO$ and DMF.

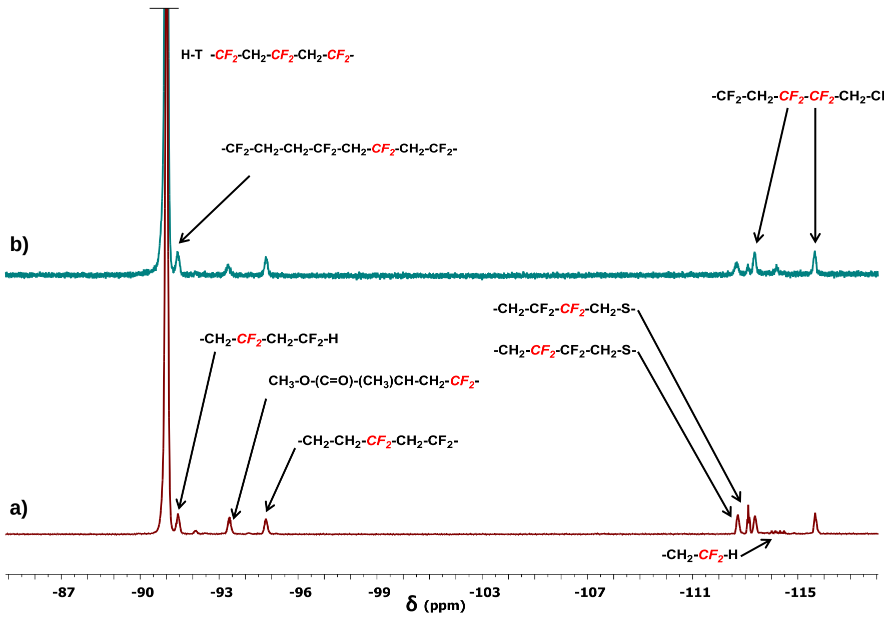

Figure S2. [19]F NMR spectra in $(CD_3)_2CO$ of: a) N_3-$PVDF_{40}$-XA and b) $PVDF_{40}$-*b*-$PDMAEMA_{23}$ BCP. H-T stands for head-to-tail.

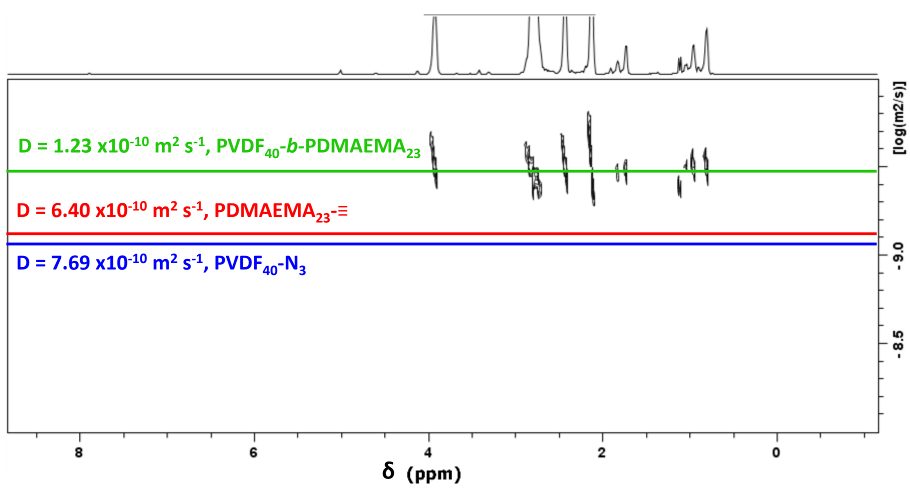

Figure S3. DOSY [1]H NMR spectrum in $(CD_3)_2CO$ of $PVDF_{40}$-*b*-$PDMAEMA_{23}$ BCP (green line and black contours). The other colored lines correspond to the diffusion coefficients of the N_3-$PVDF_{40}$-XA (blue line) and ≡-PDMAEMA-Cl (red line) building blocks. The [1]H DOSY NMR spectra of these precursors are displayed in Figure S4.

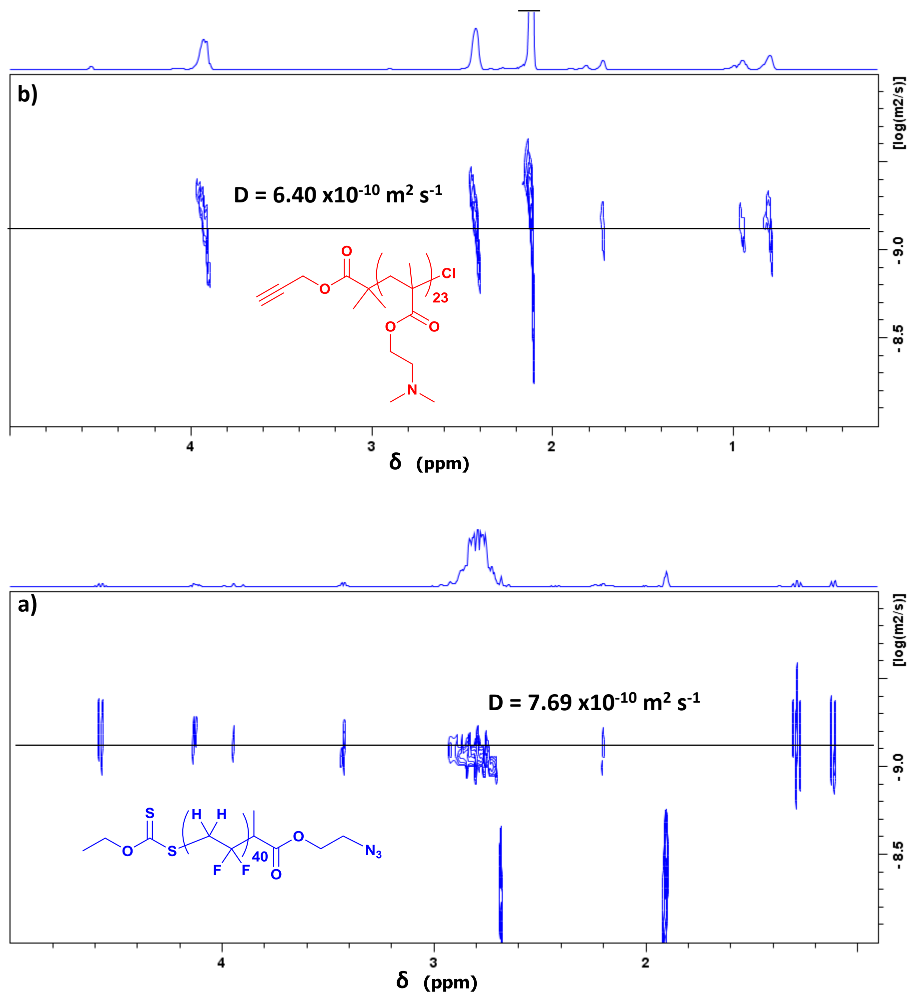

Figure S4. DOSY ^{1}H NMR spectra in $(CD_3)_2CO$ of: a) N_3-PVDF$_{40}$-XA, and b) ≡-PDMAEMA-Cl.

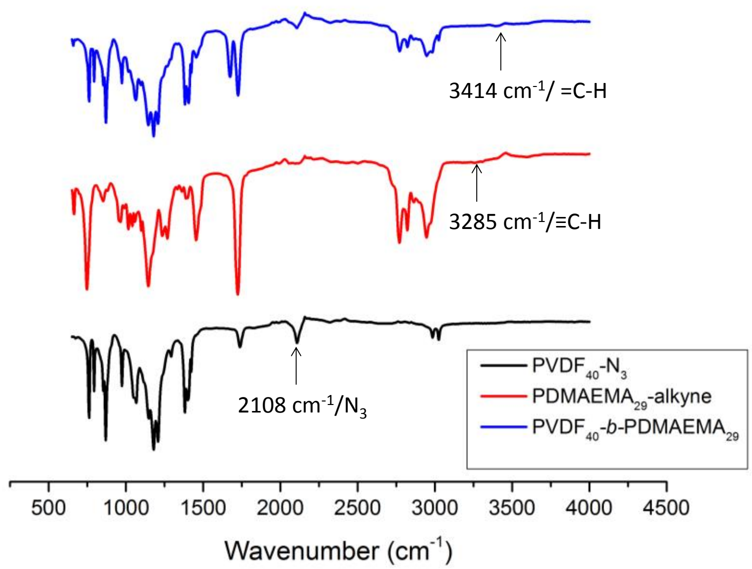

Figure S5. FTIR spectra of $PVDF_{40}$-N_3 (black trace), ≡-$PDMAEMA_{29}$ (red trace) and of the resulting $PVDF_{40}$-*b*-$PDMAEMA_{29}$ BCP (blue trace).

$PVDF_{40}$-*b*-$PDMAEMA_{79}$

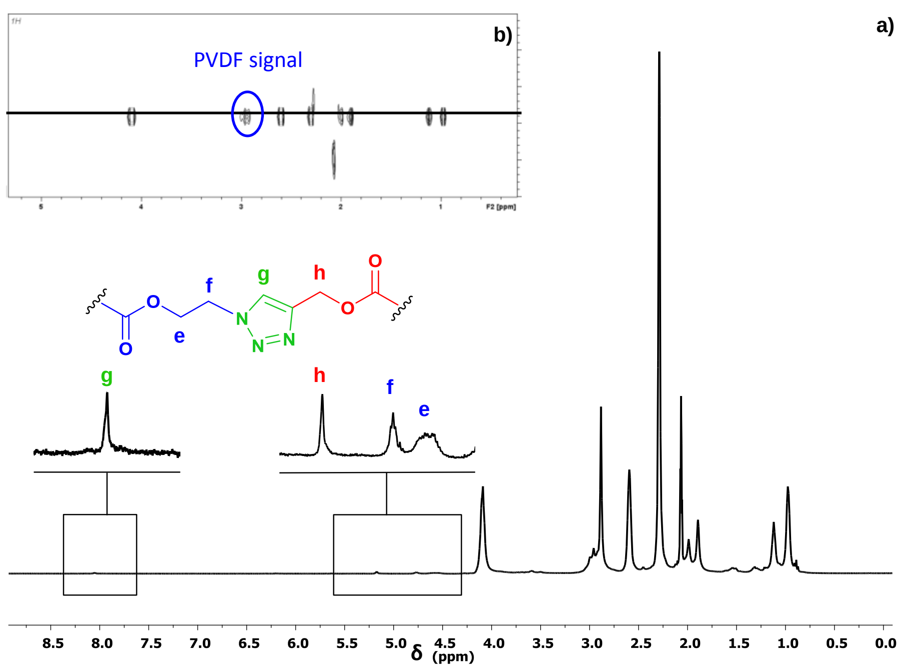

Figure S6. a) ^1H NMR spectrum in $(CD_3)_2CO$ of $PVDF_{40}$-*b*-$PDMAEMA_{79}$ BCP, b) DOSY ^1H NMR spectrum of $PVDF_{40}$-*b*-$PDMAEMA_{79}$ BCP.

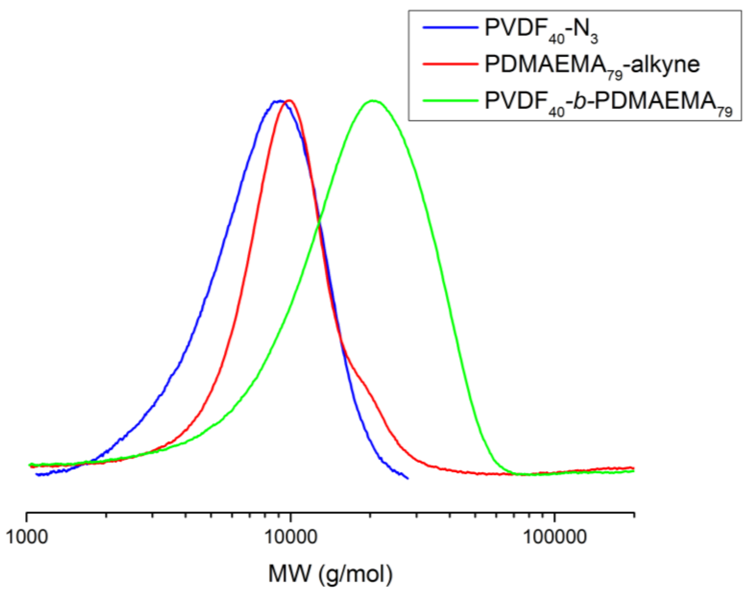

Figure S7. SEC chromatograms of $PVDF_{40}$-N_3, ≡-$PDMAEMA_{79}$ and of the resulting $PVDF_{40}$-*b*-$PDMAEMA_{79}$ BCP.

$PVDF_{40}$-*b*-$PDMAEMA_{162}$

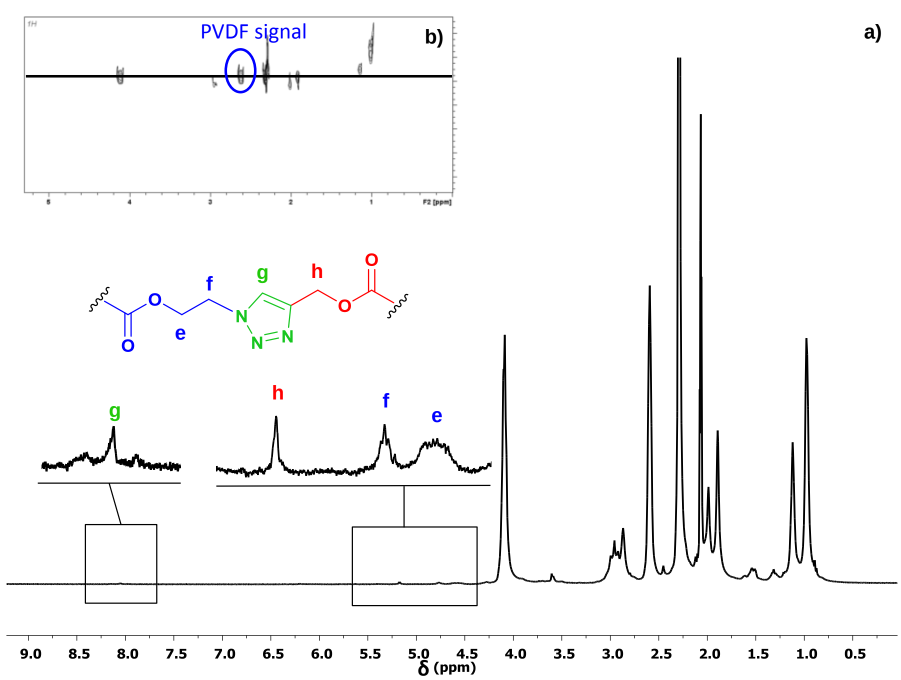

Figure S8. a) ^{1}H NMR spectrum in $(CD_3)_2CO$ of $PVDF_{40}$-*b*-$PDMAEMA_{162}$ BCP, b) DOSY ^{1}H NMR spectrum of $PVDF_{40}$-*b*-$PDMAEMA_{162}$ BCP.

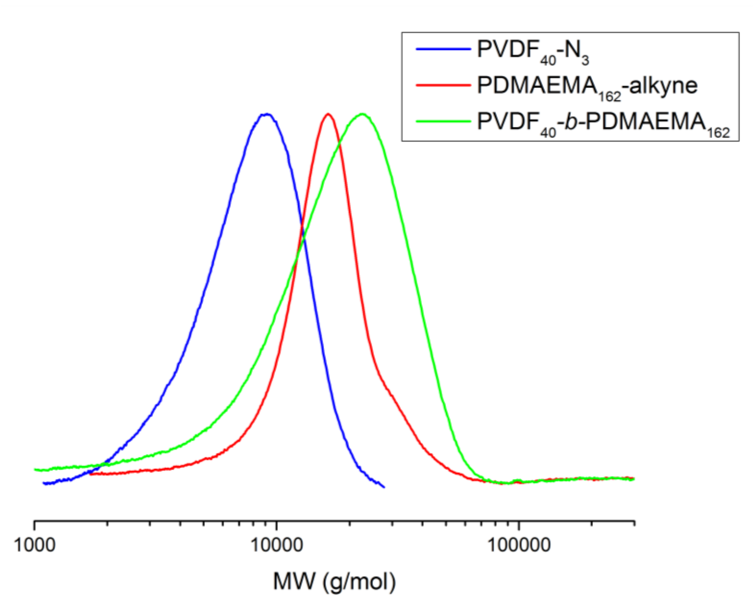

Figure S9. SEC chromatograms of $PVDF_{40}$-N_3, of ≡-$PDMAEMA_{162}$ and of the resulting $PVDF_{40}$-*b*-$PDMAEMA_{162}$ BCP.

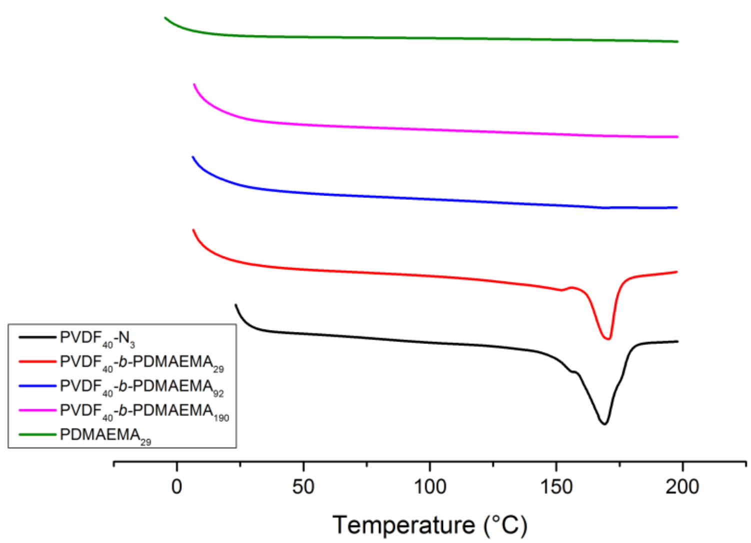

Figure S10. DSC thermograms (second heating) of $PVDF_{40}$-N_3 (black trace), $PVDF_{40}$-*b*-$PDMAEMA_{29}$ (red trace), $PVDF_{40}$-*b*-$PDMAEMA_{69}$ (blue trace), $PVDF_{40}$-*b*-$PDMAEMA_{162}$ (pink trace), and $PDMAEMA_{29}$ (green trace).

Table S1. Final concentration, pH and quaternization extent of the PVDF-*b*-PDMAEMA block copolymers.

Self-assembly target pH	Final Concentration (mg/ml) pH	$PVDF_{40}$-*b*-$PDMAEMA_{23}$	$PVDF_{40}$-*b*-$PDMAEMA_{69}$	$PVDF_{40}$-*b*-$PDMAEMA_{162}$
2	Conc (mg/ml)	4.89	5.95	4.75
	pH	1.94	2.01	2.03
Native (ca. 8)	Conc (mg/ml)	2.23	3.95	3.38
	pH	7.70	7.94	8.29
10	Conc (mg/ml)	3.64	4.18	3.85
	pH	9.51	9.51	9.53

Table S2. Intensity-average hydrodynamic diameters and PDI of PVDF-*b*-PDMAEMA amphiphilic block copolymers self-assembled in water at pH = 2, 8 and 10.

Self-assembly target pH	Intensity average hydrodynamic diameter (nm) and PDI	$PVDF_{40}$-*b*-$PDMAEMA_{23}$	$PVDF_{40}$-*b*-$PDMAEMA_{69}$	$PVDF_{40}$-*b*-$PDMAEMA_{162}$
2	Av. Diameter (nm)	239	237	279
	PDI	0.14	0.21	0.22
Native (ca. 8)	Av. Diameter (nm)	285	287	334
	PDI	0.24	0.33	0.37
10	Av. Diameter (nm)	200	139	177
	PDI	0.16	0.24	0.27

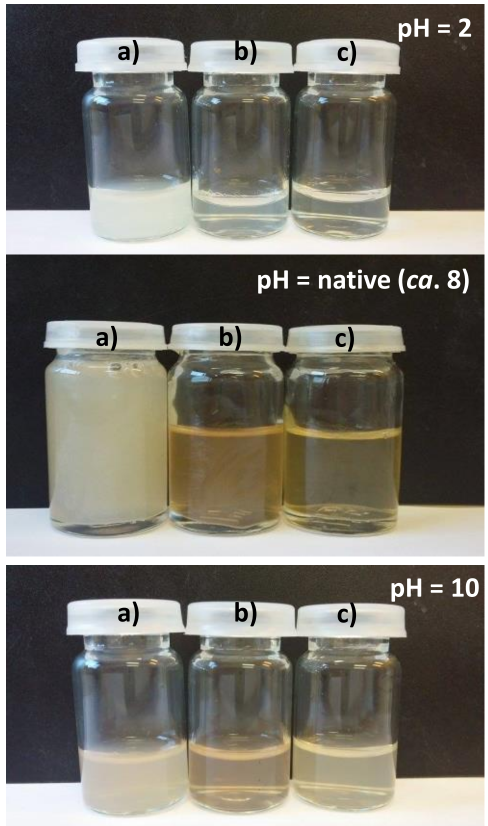

Figure S11. Macroscopic aspects of: a) $PVDF_{40}$-*b*-$PDMAEMA_{23}$, b) $PVDF_{40}$-*b*-$PDMAEMA_{69}$, and c) $PVDF_{40}$-*b*-$PDMAEMA_{162}$ self-assembled dispersions in water

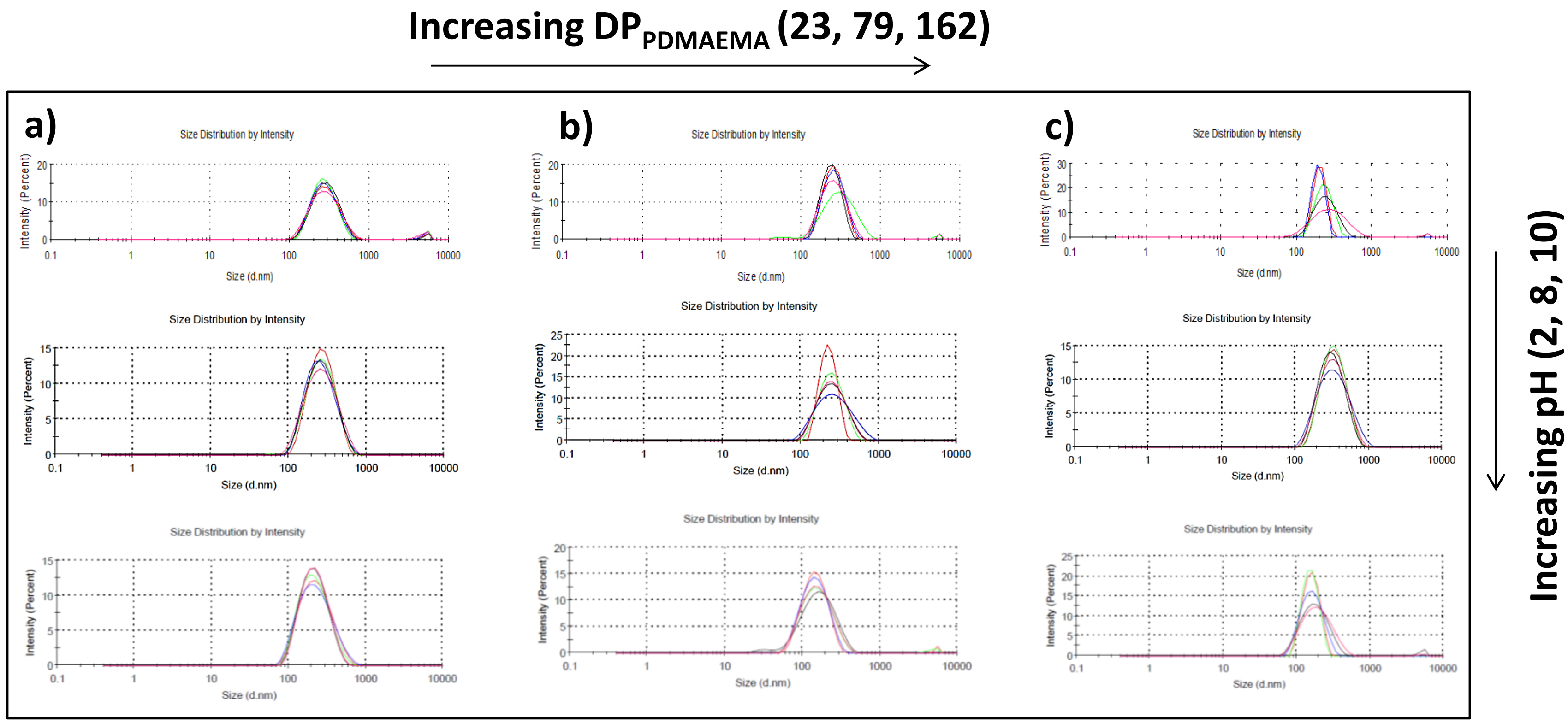

Figure S12. Comparison of intensity-average hydrodynamic diameter distributions of :a) $PVDF_{40}$-*b*-$PDMAEMA_{23}$, b) $PVDF_{40}$-*b*-$PDMAEMA_{69}$, and c) $PVDF_{40}$-*b*-$PDMAEMA_{162}$ amphiphilic block copolymers self-assembled in water at pH = 2, 8 and 10.

Note: All the BCPs suspensions appeared to have roughly the same intensity average hydrodynamic diameter measured by DLS. However, the suspensions obtained from BCP with short PDMAEMA block appear much more turbid compared to the other suspensions. This may not be surprising. DLS measures the hydrodynamic diameter which takes into account the soluble stabilizing PDMAEMA corona. If all the particles contained in these suspensions appear to have the same intensity average hydrodynamic diameter despite the length of the PDMAEMA block, it derives that their PVDF insoluble cores have to increase with decreasing PDMAEMA block length. These larger insoluble PVDF cores are responsible for the turbidity.

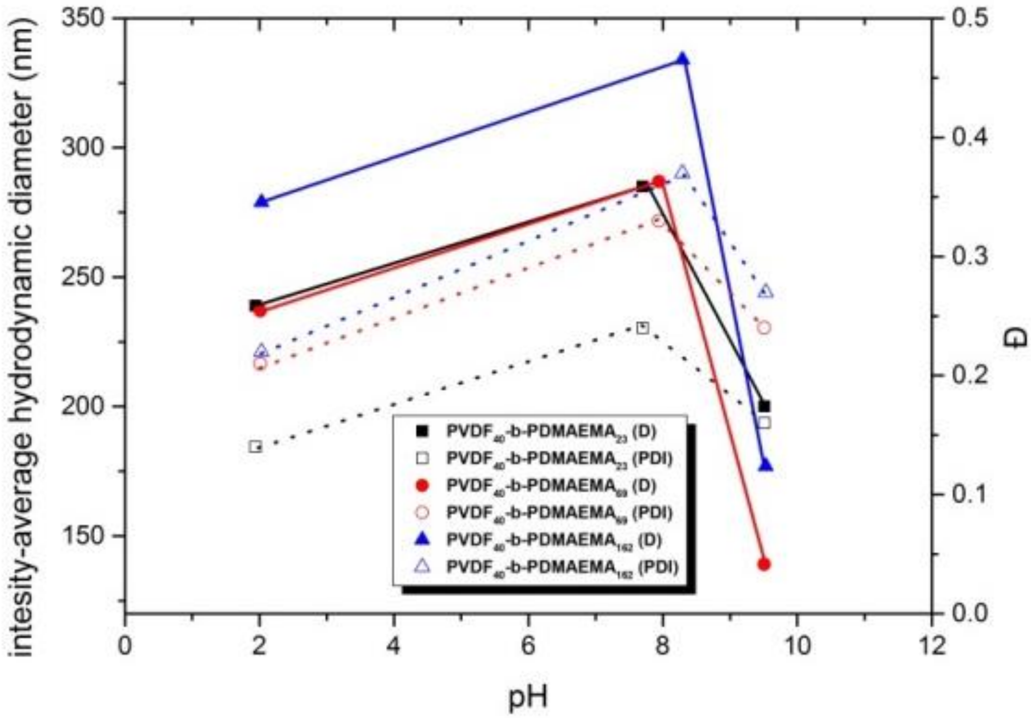

Figure S13. Evolution of the intensity-average hydrodynamic diameter and of the dispersity of PVDF-*b*-PDMAEMA amphiphilic block copolymers self-assembled nano-objects versus pH of the dispersions.

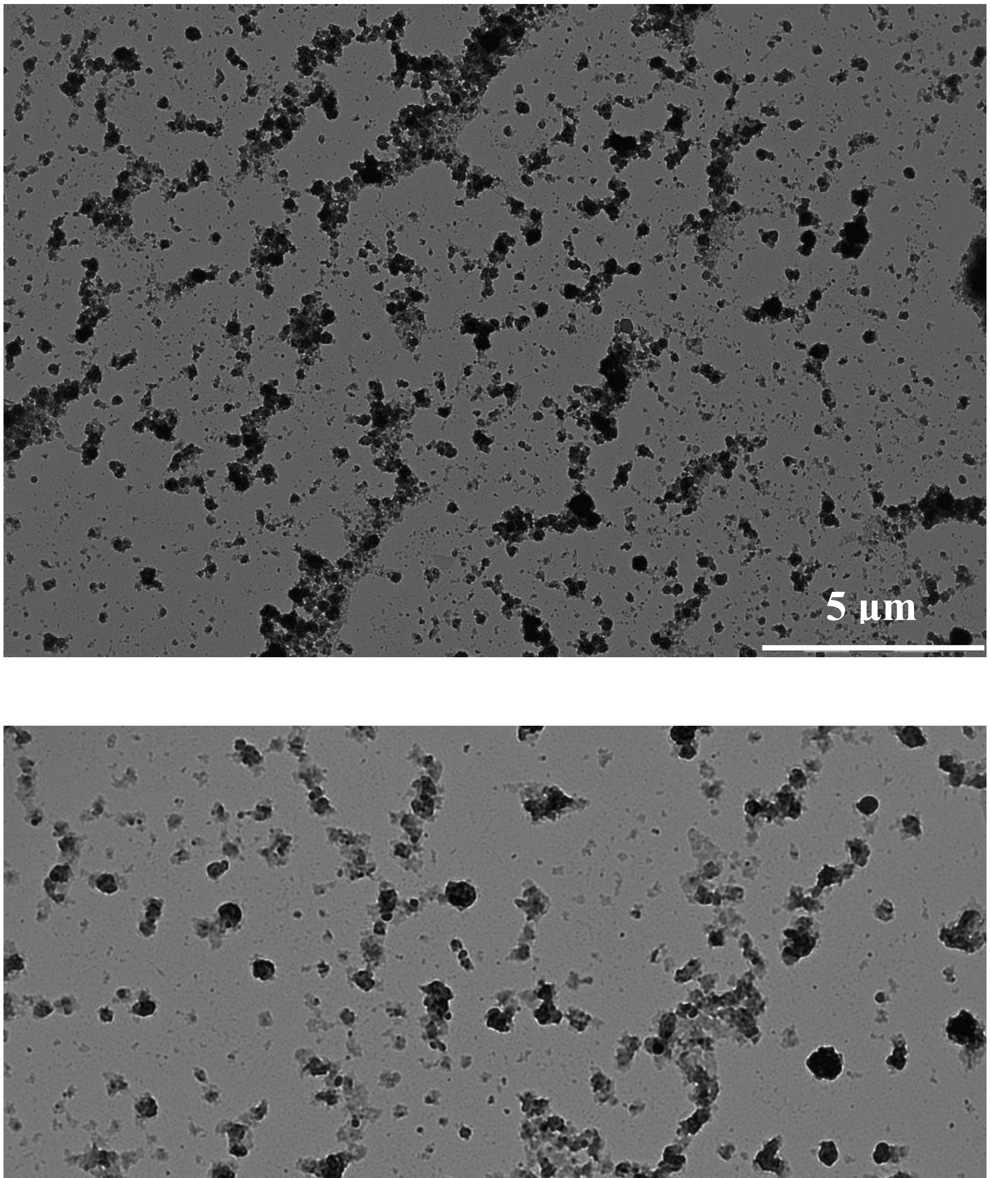

Figure S14. TEM images of $PVDF_{40}$-*b*-$PDMAEMA_{23}$ amphiphilic block copolymers self-assembled in water. (pH = 2)

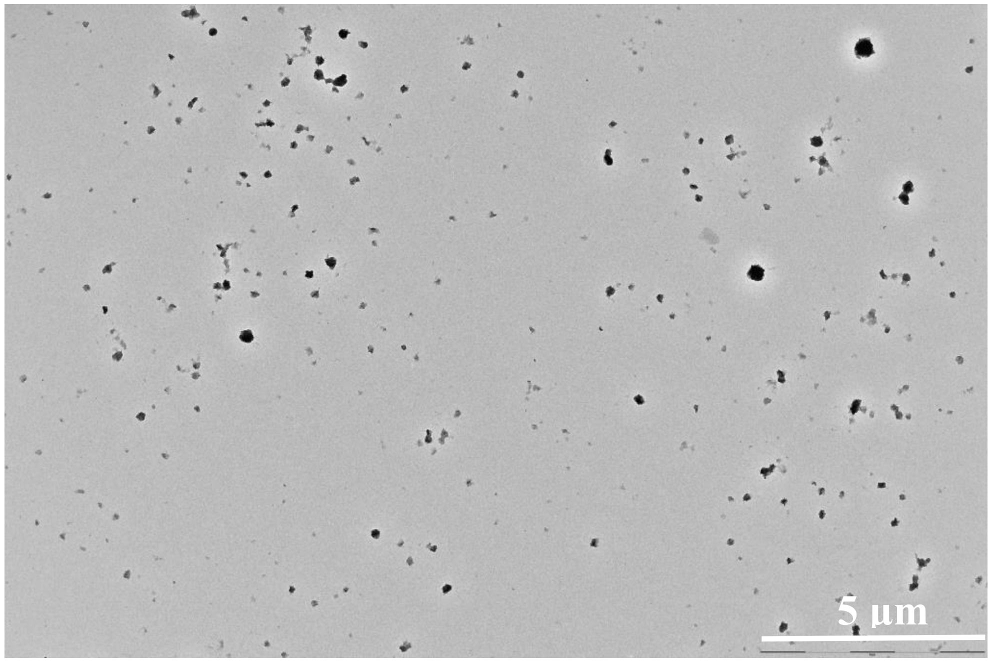

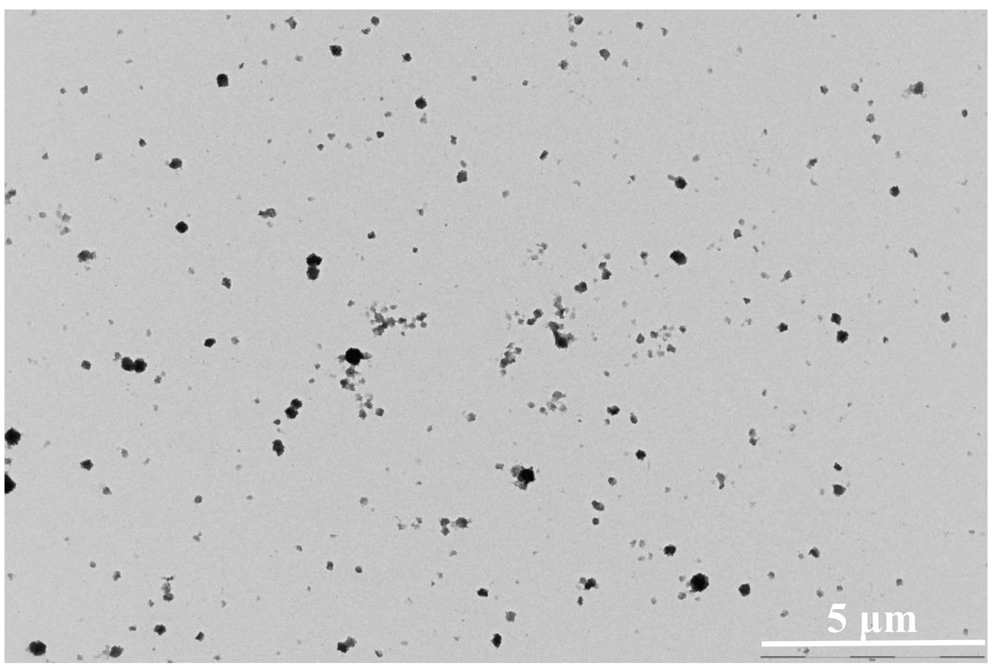

Figure S15. TEM images of $PVDF_{40}$-*b*-$PDMAEMA_{23}$ amphiphilic block copolymers self-assembled in water (pH = 8).

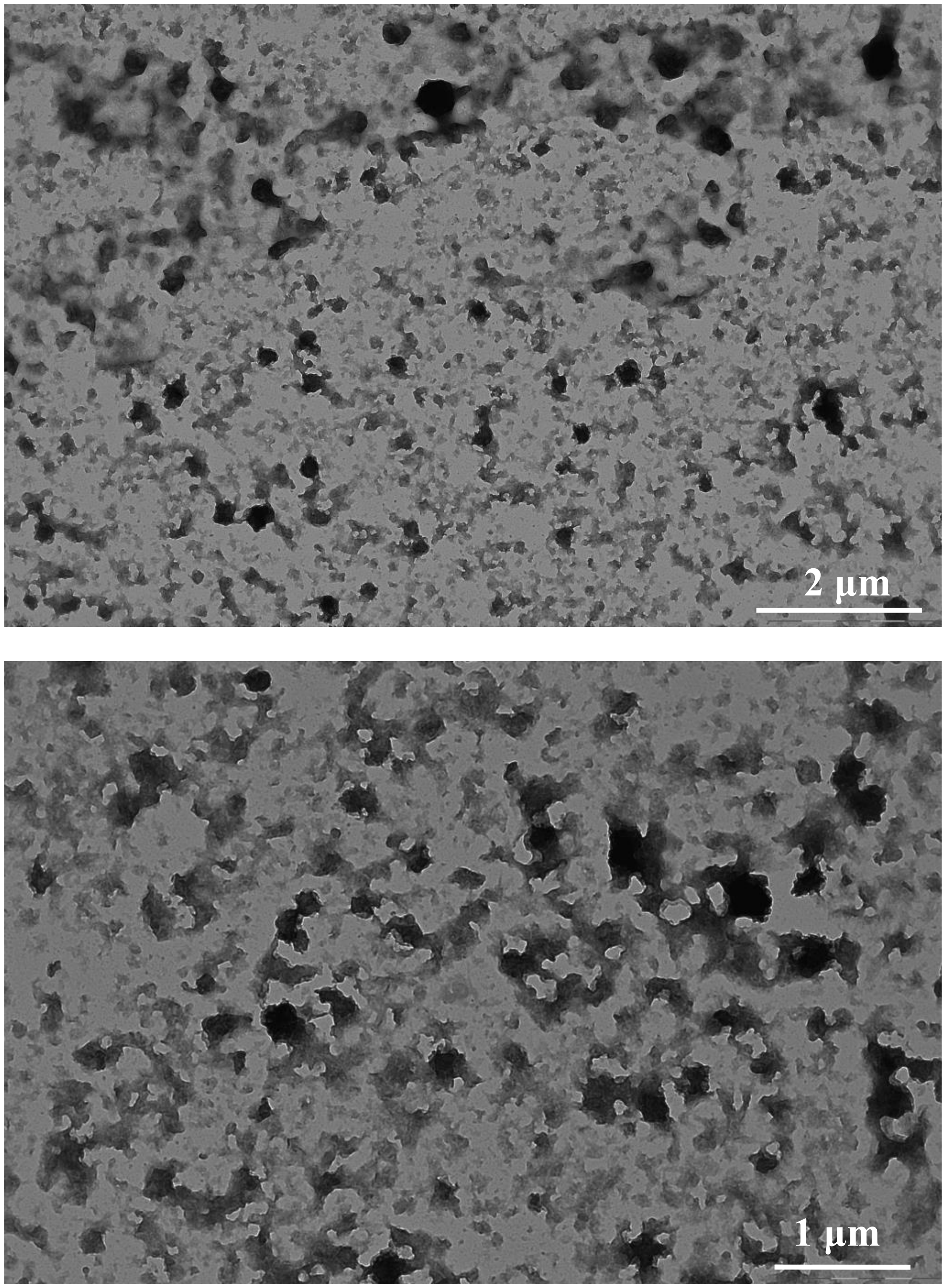

Figure S16. TEM images of $PVDF_{40}$-*b*-$PDMAEMA_{23}$ amphiphilic block copolymers self-assembled in water (pH = 10).

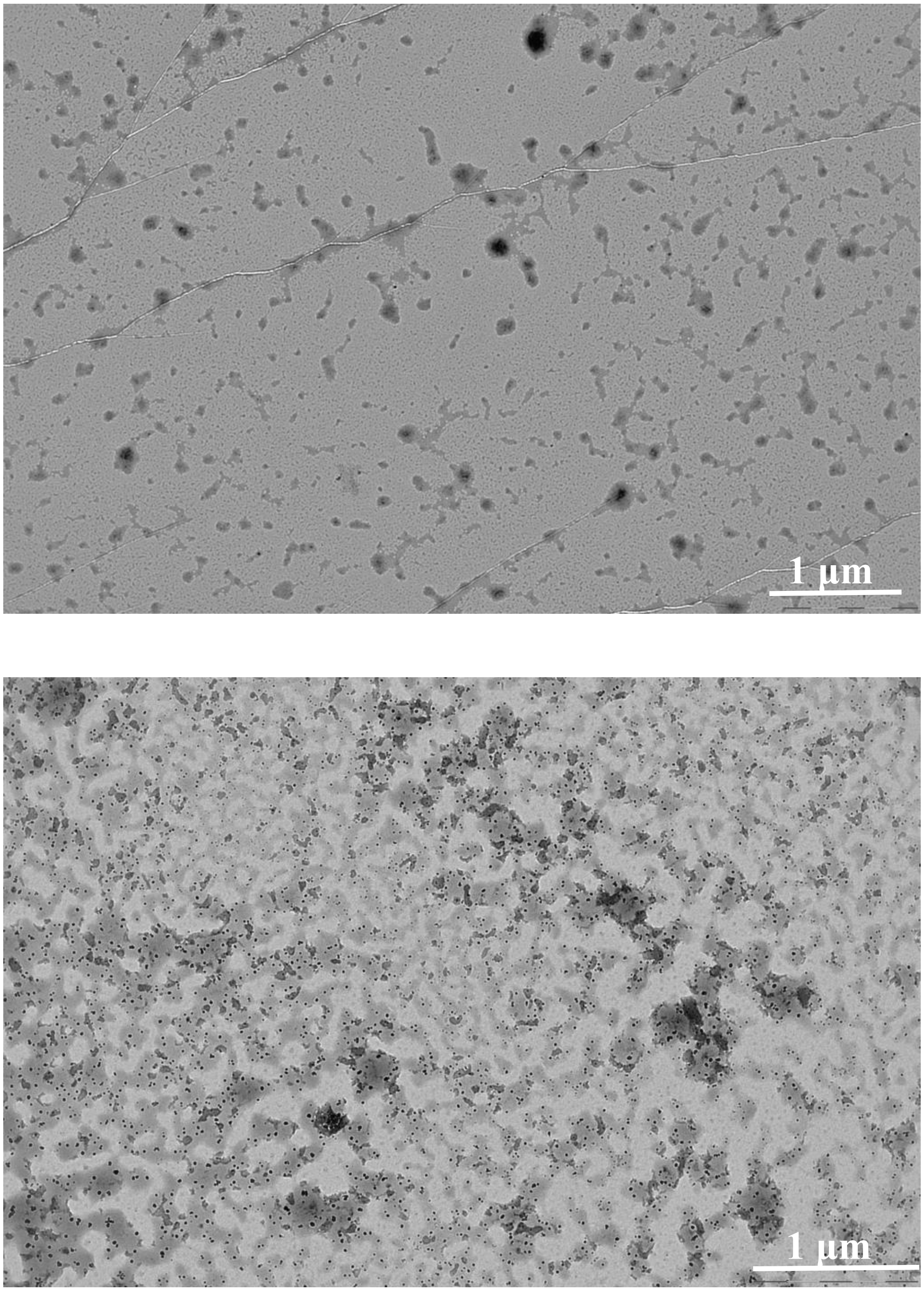

Figure S17. TEM images of PVDF$_{40}$-*b*-PDMAEMA$_{69}$ amphiphilic block copolymers self-assembled in water (pH = 2).

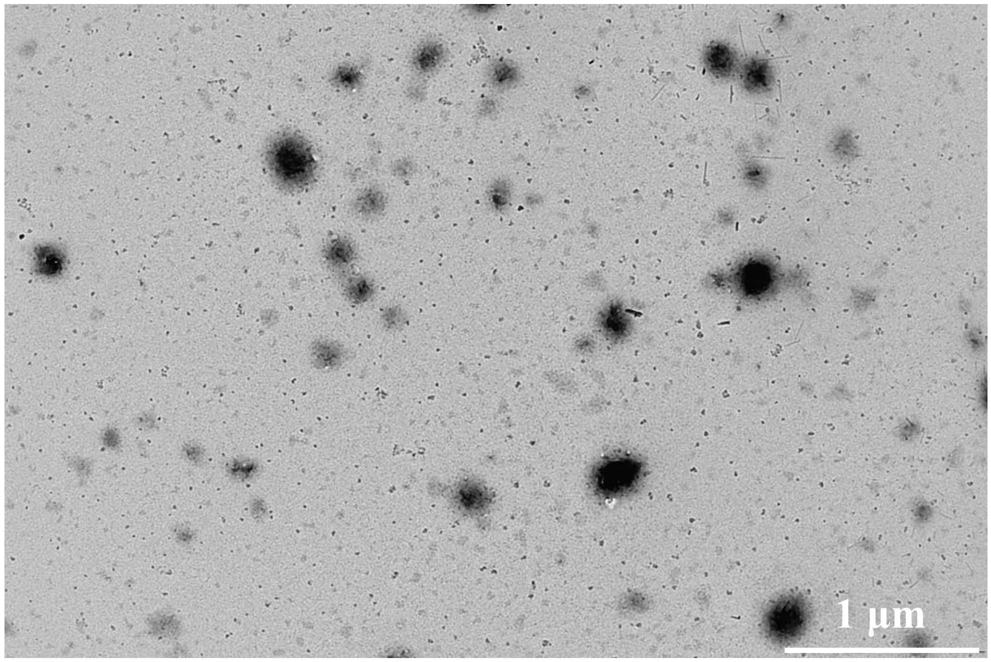

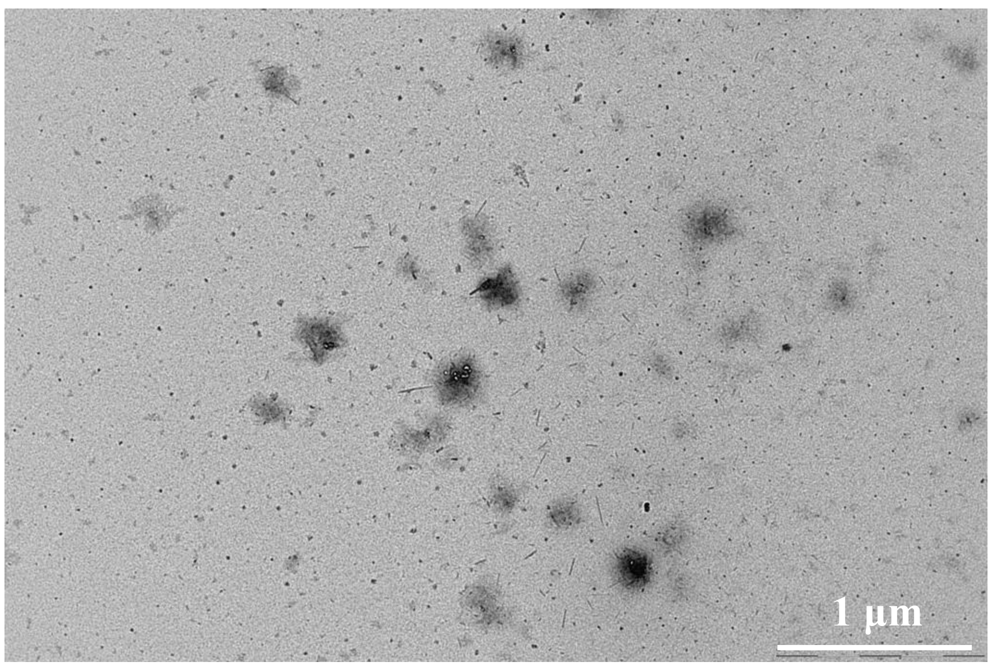

Figure S18. TEM images of $PVDF_{40}$-*b*-$PDMAEMA_{69}$ amphiphilic block copolymers self-assembled in water (pH = 8).

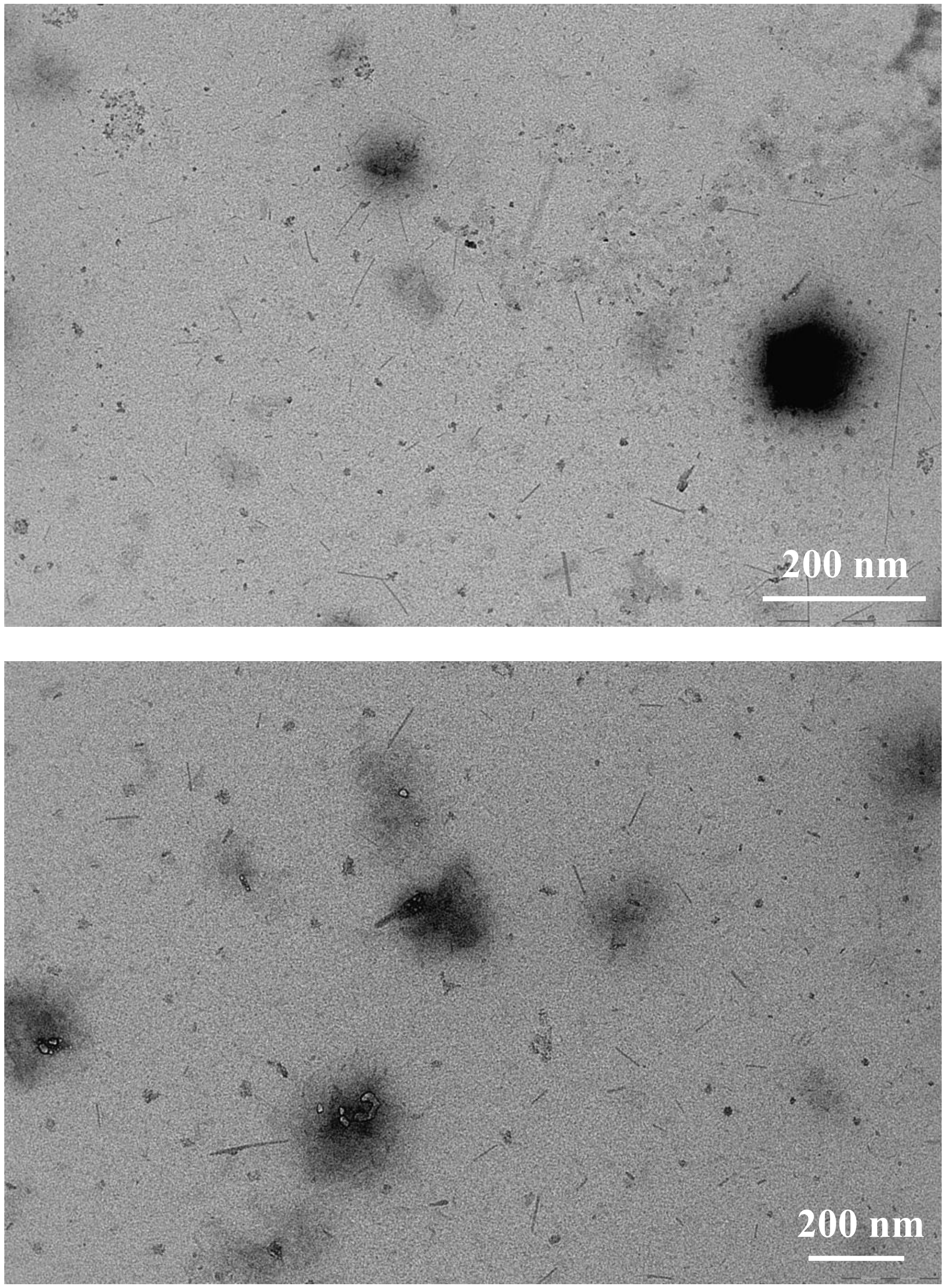

Figure S19. TEM images of $PVDF_{40}$-*b*-$PDMAEMA_{69}$ amphiphilic block copolymers self-assembled in water, zoom on rod morphologies (pH = 8).

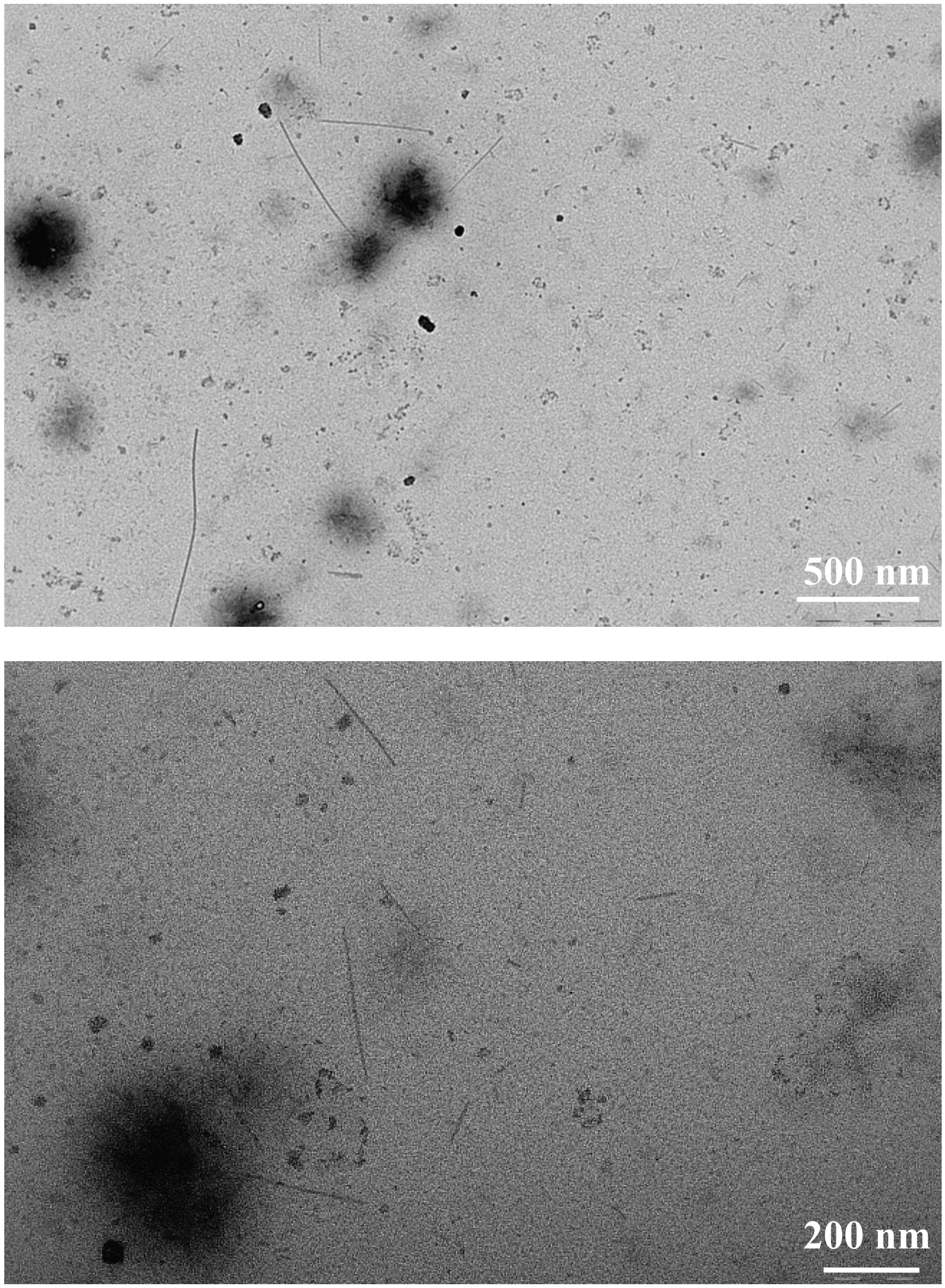

Figure S20. TEM images of $PVDF_{40}$-*b*-$PDMAEMA_{69}$ amphiphilic block copolymers self-assembled in water, zoom on rod morphologies (pH = 8).

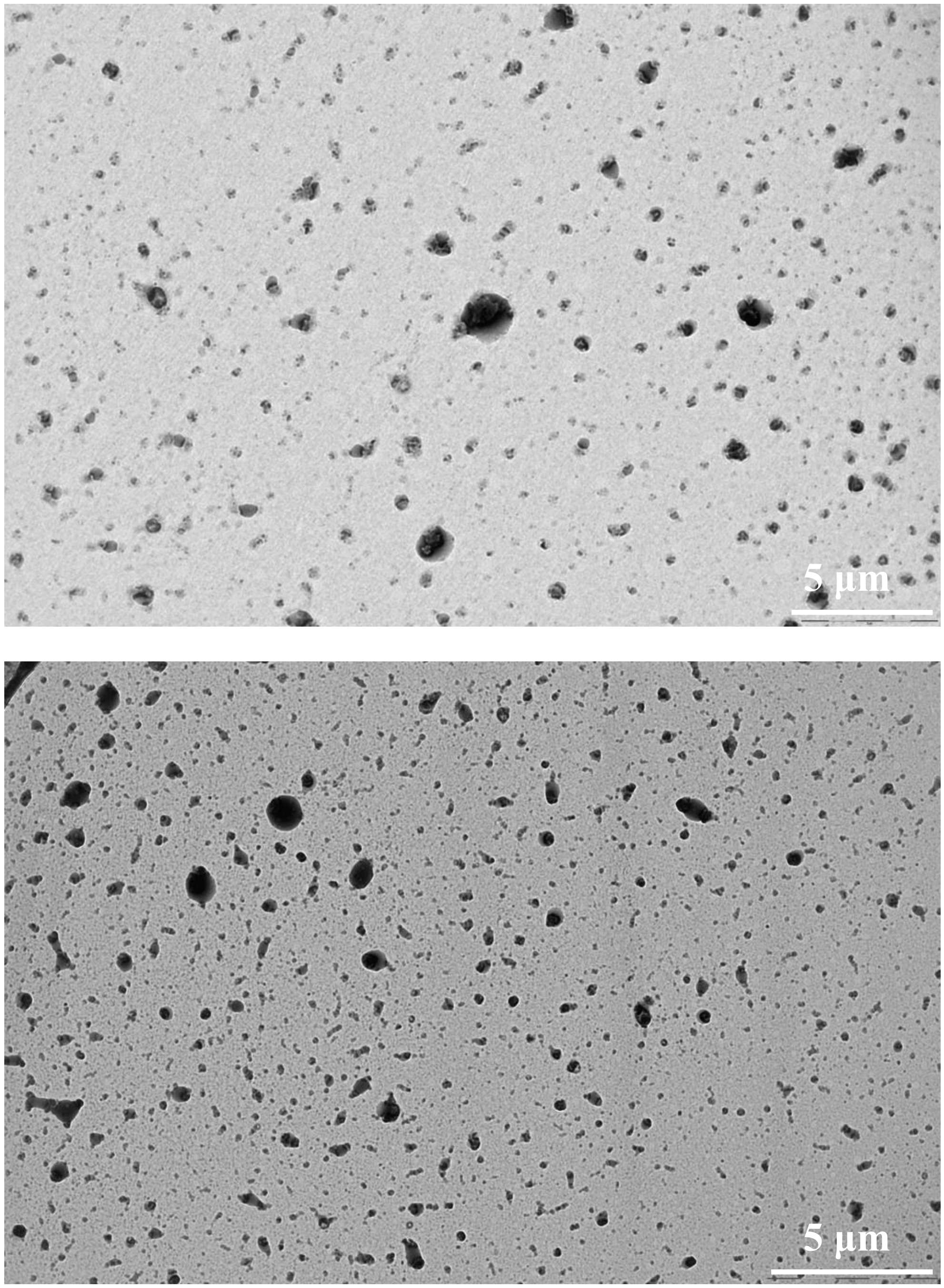

Figure S21. TEM images of $PVDF_{40}$-*b*-$PDMAEMA_{69}$ amphiphilic block copolymers self-assembled in water (pH = 10).

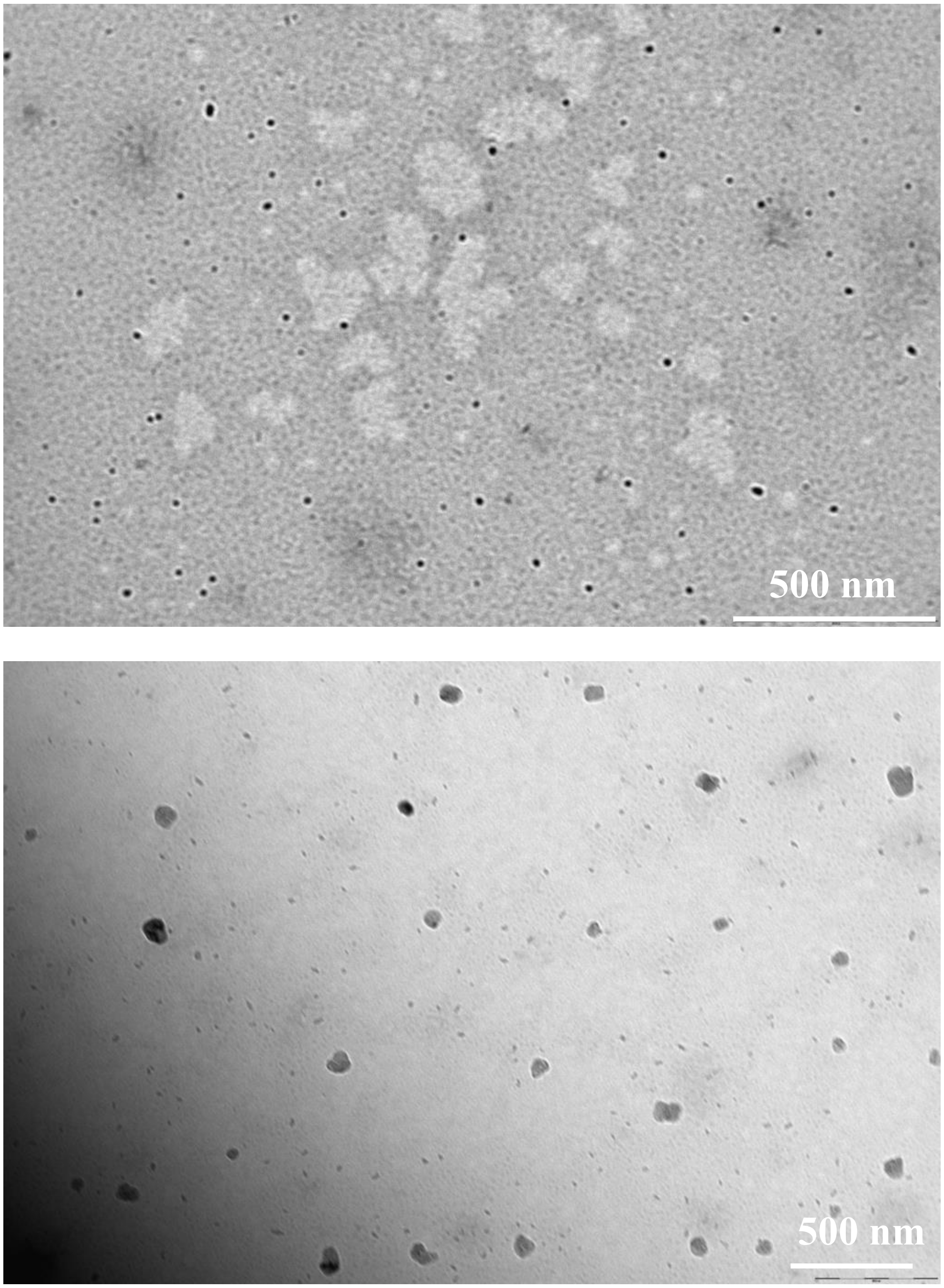

Figure S22. TEM images of $PVDF_{40}$-*b*-$PDMAEMA_{162}$ amphiphilic block copolymers self-assembled in water (pH = 2).

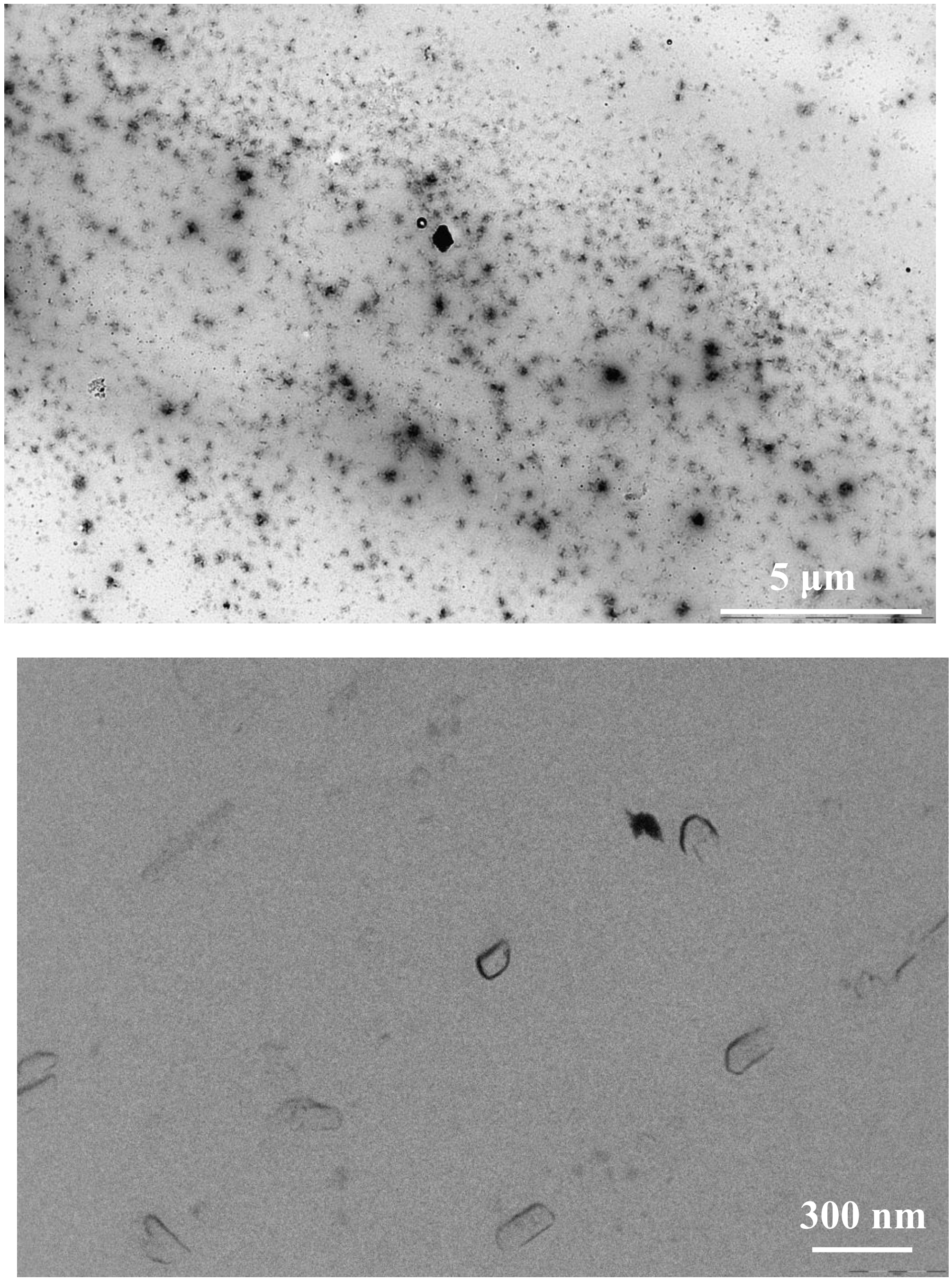

Figure S23. TEM images of $PVDF_{40}$-*b*-$PDMAEMA_{162}$ amphiphilic block copolymers self-assembled in water, zoom on ring morphologies (pH = 8).

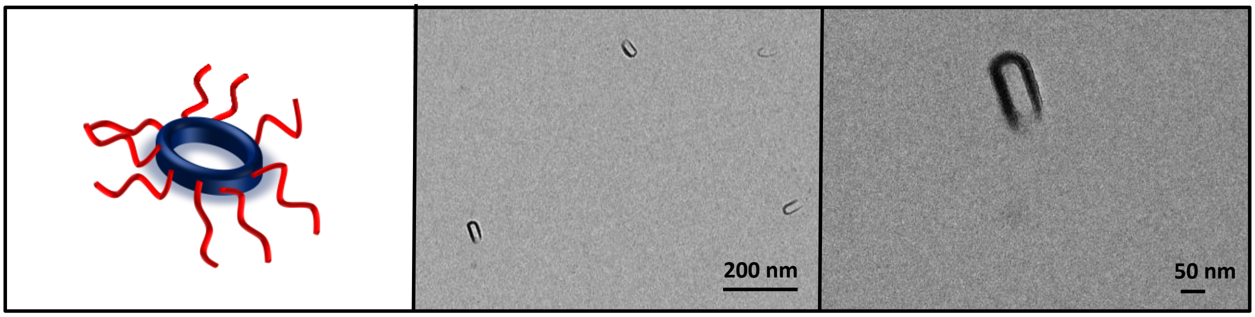

Figure S24. TEM morphologies of $PVDF_{40}$-*b*-$PDMAEMA_{162}$ amphiphilic block copolymers self-assembled in water, zoom on ring morphologies (pH = 8).

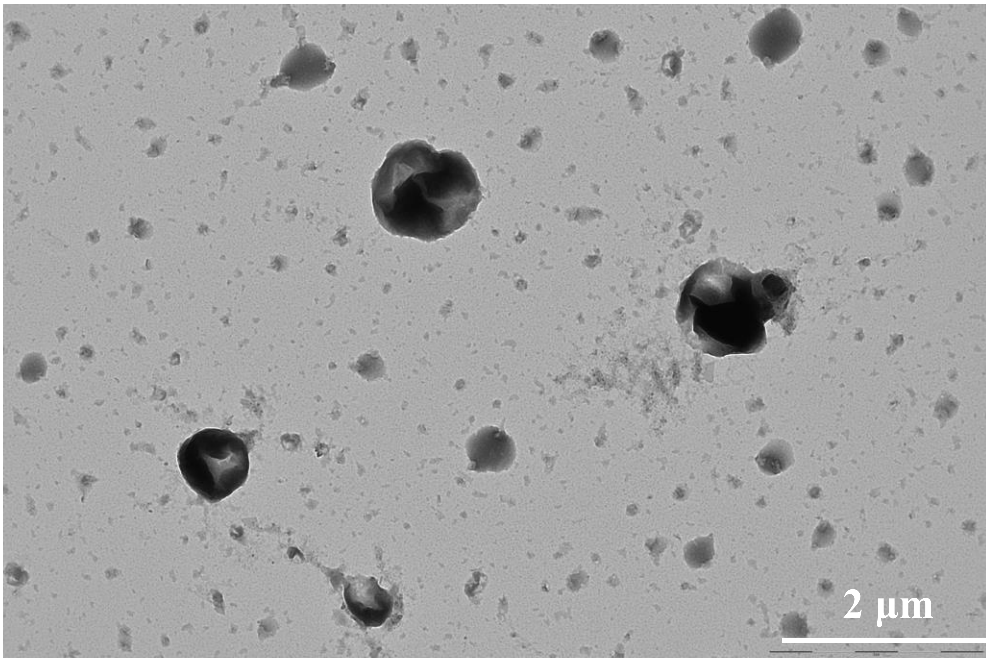

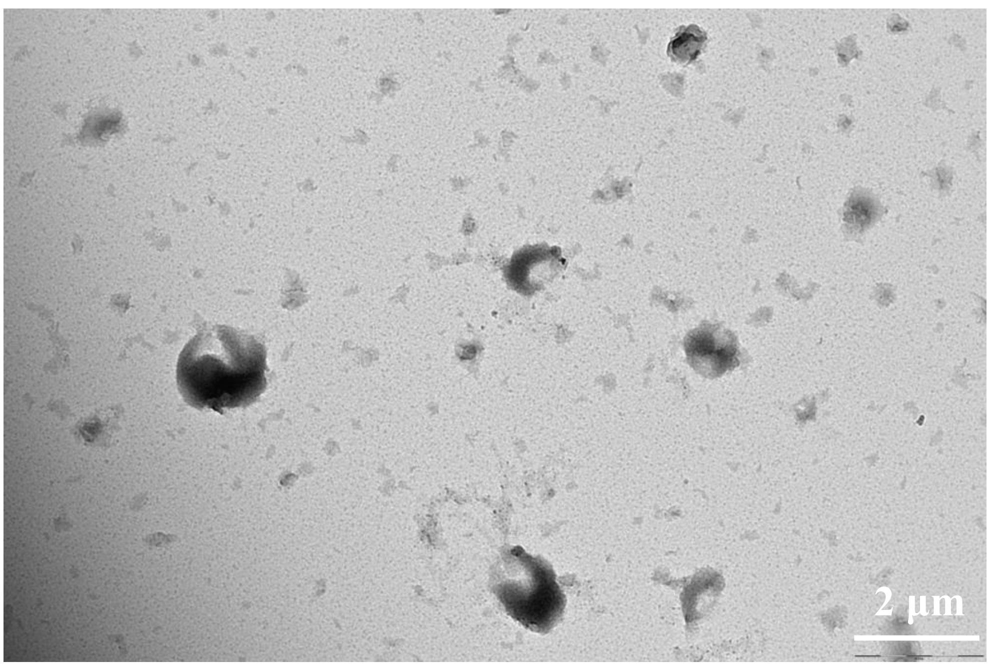

Figure S25. TEM images of $PVDF_{40}$-*b*-$PDMAEMA_{162}$ amphiphilic block copolymers self-assembled in water (pH = 10).

References:

[1] C. Barner-Kowollik, *Handbook of RAFT Polymerization*; Wiley-VCH: Weinheim, Germany, 2008.